P2Y receptor regulation of sodium transport in human mammary epithelial cells

So Yeong Lee, Melissa L. Palmer, Peter J. Maniak, Soo Hwa Jang, Pan Dong Ryu and Scott M. O'Grady

Am J Physiol Cell Physiol 293:1472-1480, 2007. First published Aug 22, 2007;
doi:10.1152/ajpcell.00068.2007

Am J Physiol Cell Physiol 293: C1472–C1480, 2007.
First published August 22, 2007; doi:10.1152/ajpcell.00068.2007.

P2Y receptor regulation of sodium transport in human mammary epithelial cells

So Yeong Lee,[1] Melissa L. Palmer,[2] Peter J. Maniak,[2] Soo Hwa Jang,[1] Pan Dong Ryu,[1] and Scott M. O'Grady[2]

[1]*Department of Veterinary Pharmacology, College of Veterinary Medicine, Seoul National University, Seoul, South Korea; and* [2]*Departments of Physiology and Animal Science, University of Minnesota, St. Paul, Minnesota*

Submitted 18 February 2007; accepted in final form 9 August 2007

Lee SY, Palmer ML, Maniak PJ, Jang SH, Ryu PD, O'Grady SM. P2Y receptor regulation of sodium transport in human mammary epithelial cells. *Am J Physiol Cell Physiol* 293: C1472–C1480, 2007. First published August 22, 2007; doi:10.1152/ajpcell.00068.2007.— Primary human mammary epithelial (HME) cells were immortalized by stable, constitutive expression of the catalytic subunit of human telomerase. Purinergic receptors were identified by RT-PCR and quantitative RT-PCR from mRNA isolated from primary and immortalized cells grown to confluence on membrane filters. Several subtypes of P2Y receptor mRNA were identified including $P2Y_1$, $P2Y_2$, $P2Y_4$, and $P2Y_6$ receptors. RT-PCR experiments also revealed expression of A_{2b} adenosine receptor mRNA in primary and immortalized cells. Confluent monolayers of HME cells exhibited a basal short-circuit current (I_{sc}) that was abolished by amiloride and benzamil. When monolayers were cultured in the presence of hydrocortisone, mRNA expression of Na^+ channel (ENaC) α-, β-, and γ-subunits increased approximately threefold compared with that in cells grown without hydrocortisone. In addition, basal benzamil-sensitive Na^+ transport was nearly twofold greater in hydrocortisone-treated monolayers. Stimulation with UTP, UDP, or adenosine 5′-*O*-(3-thiotriphosphate) (ATPγS) produced increases in intracellular calcium concentration that were significantly reduced following pretreatment with the calcium-chelating agent BAPTA-AM. Concentration-response relationships indicated that the rank order of potency for these agonists was UTP > UDP > ATPγS. Basolateral stimulation with UTP produced a rapid but transient increase in I_{sc} that was significantly reduced if cells were pretreated with BAPTA-AM or benzamil. Moreover, basolateral treatment with either charybdotoxin or clotrimazole significantly inhibited the initial UTP-dependent increase in I_{sc} and eliminated the sustained current response. These results indicate that human mammary epithelial cells express multiple P2 receptor subtypes and that Ca^{2+} mobilization evoked by P2Y receptor agonists stimulates Na^+ absorption by increasing the activity of Ca^{2+}-activated K^+ channels located in the basolateral membrane.

adenosine receptors; epithelial sodium channels; KCNN4; SK4; potassium channels

THE MAMMARY GLAND is composed of multiple cell types, which include acinar and duct epithelial cells, myoepithelial cells, and stromal cells (31). The functional secretory structure of the human mammary gland is known as the terminal ductal lobular unit, which is composed of a cluster of lobules and acini that emerge from the terminal duct. The duct is composed of epithelial cells that surround a central lumen (luminal epithelial cells) and express a variety of cytokeratins, including cytokeratin 18 (11, 31). Growth and differentiation of the mammary epithelium is subject to regulation by steroid hormones including estrogen and progesterone, the lactogenic hormone prolactin, and growth factors that are released by the adjacent stromal cells (9, 19, 24). Epithelial-stromal cell interactions influence mammary gland growth and development, highlighting the importance of paracrine regulation occurring with age and reproductive state (24).

In a previous study, normal human mammary epithelial (HME) cells obtained from a 51-yr-old woman were immortalized following transfection with a plasmid containing the human telomerase (hTERT) catalytic subunit (17). A single copy of the exogenous hTERT gene was expressed in the later passages of HME cells where telomere length was shown to be extended and stabilized without the activation of endogenous hTERT or c-Myc genes. In addition, immortalized HME cells exhibited a loss of $p16^{INK4a}$ expression, which is known to be associated with increased phosphorylation of Rb protein and subsequent repression of an important cell cycle checkpoint. Life span extension of HME cells beyond *passage 123* was documented with average population doubling times of 0.78 and 0.93 days depending on media conditions. Although previous experiments involving HME cells provided a detailed characterization of the growth properties and expression patterns of cell cycle regulatory proteins, no physiological characterization was reported.

In the present study, we investigated electrolyte transport in these cells and its regulation by purinergic receptor agonists. Our results revealed that HME cells express a variety of purinergic receptors that are known to play important roles in both autocrine and paracrine regulation of transport function in epithelia (4, 6, 7). In particular, a recent study using mouse mammary epithelial cells demonstrated that ATP and UTP increase anion and fluid secretion and suggested that purinergic receptor activation may be involved in fibrocystic disease occurring in premenopausal women (3). The major objectives of this study were to *1*) identify purinoceptor subtypes expressed in HME cells, *2*) examine the effects of P2Y receptor stimulation on transport properties of the epithelium, and *3*) determine the molecular identity of ion channels involved in P2Y receptor regulation of transport function in these cells. Our results indicated that, in contrast to previous studies of mouse or bovine mammary epithelial cells or human mammary tumor cells, HME cells exhibited a basal ENaC-dependent Na^+ absorption that was stimulated by basolateral application of UTP. Moreover, this increase in Na^+ transport was dependent

Address for reprint requests and other correspondence: S. M. O'Grady, Dept. of Physiology, 495 Animal Science/Veterinary Medicine Bldg., Univ. of Minnesota, 1988 Fitch Ave., St. Paul, MN 55108 (e-mail: ograd001@umn.edu).

The costs of publication of this article were defrayed in part by the payment of page charges. The article must therefore be hereby marked "*advertisement*" in accordance with 18 U.S.C. Section 1734 solely to indicate this fact.

on mobilization of intracellular Ca^{2+} and activation of basolateral K^+ channels that were blocked by inhibitors of KCNN4.

MATERIALS AND METHODS

Materials. UTP, 17β-estradiol, and hexokinase were purchased from Sigma-Aldrich (St. Louis, MO). 8-(4-Chlorophenylthio)adenosine 3′,5′-cyclic monophosphate was purchased from RBI (Natick, MA). $P2Y_1$ and $P2Y_2$ receptor antibodies were obtained from Alomone Laboratories (Jerusalem, Israel). Primary HME cells were originally obtained from a normal 51-yr-old woman and purchased from Clonetics (San Diego CA). Mammary epithelium growth medium (MEGM) was purchased from Clonetics along with a factor growth supplement kit that contained insulin (final concentration: 2.5 μg/ml), human epidermal growth factor (final concentration: 5 μg/ml), hydrocortisone (final concentration: 0.5 μg/ml), gentamicin sulfate/amphotericin B (final concentration: 0.5 ml/l), and bovine pituitary extract (final concentration: 2 ml/l). Medium used to culture T84 cells (DMEM/F12) was purchased from Cambrex Bio Science (Baltimore, MD).

Cell preparation and culture. Primary HME cells were transfected with pCI-neo-hTERT expression plasmid to achieve immortalization of the cells as described previously (23). The immortalized cells were cultured in MEGM at 37°C with 5% CO_2. T84 cells were grown in DMEM/F12 supplemented with 3.7 g/l $NaHCO_3$, 10% FBS, 10 mg/ml insulin, 1% nonessential amino acid, 5 mg/ml fungizone, 100 U/ml penicillin, 100 mg/ml streptomycin, and 100 mg/ml kanamycin (standard medium). Epithelial cell monolayers were grown on Costar Transwell permeable supports (Corning, Acton, MA) without any additional substrate and incubated at 37°C in a humidified atmosphere of 5% CO_2 in air.

Identification of P2Y receptors, A_{2b} receptor, ENaC subunits, CFTR, and KCNN4 by RT-PCR and quantitative RT-PCR. RT-PCR was used to identify purinergic receptors, epithelial Na^+ channel (ENaC) α-, β-, and γ-subunits, and CFTR from primary and immortalized HME cells. Total RNA was extracted using Trizol reagent (Invitrogen, Carlsbad, CA). Total RNA (2 μg) was reverse transcribed using random hexamer primers (Invitrogen) and the SuperScript II reverse transcription kit (Invitrogen). Primers used in this study are shown in Table 1. The initial condition was 94°C for 4 min, followed by 94°C for 45 s, annealing temperature (Table 1) for 45 s, and 72°C for 1 min for 30 cycles. All PCR products were gel purified using the QIAquick gel extraction kit (Qiagen, Valencia, CA) and sequenced using gene-specific primers to confirm the amplified sequences. DNA sequencing was performed at the Advanced Genetics Analysis Center at the University of Minnesota. Quantitative RT-PCR (QRT-PCR) reactions were carried out using SYBR green detection of newly synthesized PCR products following protocols described in QRT-PCR kits from Stratagene (Agilent Technologies, Santa Clara, CA). Fluorescence detection was performed using the Mx3005P real-time PCR system. RT reactions were performed using DNase-treated RNA samples from immortalized cells following the protocol provided by Ambion (Turbo DNase; Applied Biosystems, Foster City, CA). RT reactions were diluted 1:60 for each QRT-PCR reaction. SYBR green master mix (1:2) and passive reference dye (1:200) were purchased from Stratagene. Primers used for the QRT-PCR reactions are listed in Table 2. Efficiencies were calculated using the slope of the normalized (maximum fluorescence = 1) amplification plots divided by a twofold change in product/cycle number.

Measurement of intracellular Ca^{2+}. Cells were seeded at low density on coverslip chamber slides for 48 h in HME cell culture medium. At the start of the experiment, the cells were bathed in Hanks' balanced salt solution (HBSS) containing 10 mM HEPES buffer, pH 7.4. The cells were loaded with 10 μM fura-2 AM (Molecular Probes, Eugene, OR) for 90 min, washed in HBSS, and mounted onto the stage of a Nikon Diaphot inverted microscope with an epifluorescence attachment. Fluorescence in single cells was visualized using a Nikon UV-fluor ×40 oil-immersion objective. The fluorescence excitation, image acquisition and real-time data analyses were controlled using Image-1 Metamorph software (Universal Imaging, Westchester, PA) running on a Pentium 4 microcomputer. Intracellular Ca^{2+} concentration ($[Ca^{2+}]_i$) was measured as the ratio of fluorescence emitted at 510 nm when the cells were alternately excited at 340 and 380 nm (F_{340}/F_{380}). P2Y receptor agonists were introduced by single-pass, continuous-flow perfusion. Cells were washed with HBSS solution before addition of either a second agonist or an increase in concentration of the same agonist. $[Ca^{2+}]_i$ was calculated following calibration with the fura-2 AM calcium-imaging calibration kit (F6774) available from Molecular Probes (Eugene, OR).

Transepithelial electrical measurements. Transepithelial resistance of the cell monolayers was measured with the EVOM epithelial voltohmmeter coupled to Ag-AgCl "chopstick" electrodes [World Precision Instruments (WPI), New Haven, CT]. Measurements of

Table 1. *Forward and reverse primers for standard PCR reactions*

Standard Name (Accession No.)	Fragment Size, bp	Forward/Reverse Primers	Annealing Temperature, °C
$P2Y_1$ (U42030)	528	5′-CGGTCCGGGTTCGTCC-3′ 5′-CGGACCCCGGTACCT-3′	60
$P2Y_2$ (U07225)	638	5′-CTCTACTTTGTCACCACCAGCG-3′ 5′-TTCTGCTCCTACAGCCGAATGTCC-3′	60
$P2Y_4$ (X91852)	405	5′-CCACCTGGCATTGTCAGACACC-3′ 5′-GAGTGACCAGGCAGGGCACGC-3′	65
$P2Y_6$ (U52464)	365	5′-CGCTTCCTCTTCTATGCCAACC-3′ 5′-CCATCCTGGCGGCACAGGCGGC-3′	65
GAPDH (X02231)	410	5′-CCCTCAAGATTGTCAGCAATG-3′ 5′-GTCCTCAGTGTAGCCCAGGAT-3′	65
A_{2b} (AY136748)	299	5′-GGTCATTGCTGTCCTCTGG-3′ 5′-TCCTCGAGTGGTCCATCAG-3′	60
ENaCα (NM_001038)	257	5′-GAACAACTCCAACCTCTGGATGTC-3′ 5′-TCTTGGTGCAGTCGCCATAATC-3′	60
ENaCβ (L36593)	277	5′-TGCTGTGCCTCATCGAGTTTG-3′ 5′-TGCAGACGCAGGGAGTCATAGTTG-3′	60
ENaCγ (L36592)	237	5′-TCAAGAAGAATCTGCCCGTGAC-3′ 5′-GGAAGTGGACTTTGATGGAAACTG-3′	60
CFTR (M28668)	475	5′-AGCATTTGCTGATTGCACAG-3′ 5′-TTGCCAGGAAGCCATTTATC-3′	60

ENaC, epithelial Na^+ channel.

Table 2. *Forward and reverse primers for QRT-PCR reactions*

Standard Name (Accession No.)	Fragment Size, bp	Forward/Reverse Primers	Annealing Temperature, °C
$hP2Y_1$ (U42030)	162	5′-TTACTACCTGCCGGCTGTCT-3′ 5′-GGCAGAGTCAGCACGTACAA-3′	60
$hP2Y_2$ (U07225)	139	5′-CTGGCTGTGTCTGATGCACT-3′ 5′-TGCTGCAGTAAAGGTTGGTG-3′	60
$hP2Y_4$ (NM_002565)	146	5′-AGGCTCTGCACAGTCGTCTT-3′ 5′-GTACTCGGCAGTCAGCTTCC-3′	60
$hP2Y_6$ (NM_176797)	173	5′-ACCCACCACCTGTGTCTACC-3′ 5′-CAGCCAGAGCAAGGTTTAGG-3′	60
GAPDH (NM_002046)	177	5′-ATGACATCAAGAAGGTGGTG-3′ 5′-CATACCAGGAAATGAGCTTG-3′	56
ENaCα (NM_001038)	257	5′-GAACAACTCCAACCTCTGGATGTC-3′ 5′-TCTTGGTGCAGTCGCCATAATC-3′	60
ENaCβ (L36593)	277	5′-TGCTGTGCCTCATCGAGTTTG-3′ 5′-TGCAGACGCAGGGAGTCATAGTTG-3′	60
ENaCγ (L36592)	237	5′-TCAAGAAGAATCTGCCCGTGAC-3′ 5′-GGAAGTGGACTTTGATGGAAACTG-3′	60
CFTR (NM_000492.3)	476	5′-AGCATTTGCTGATTGCACAG-3′ 5′-TTGCCAGGAAGCCATTTATC-3′	60
hKCNN4 (NM_002250.2)	152	5′-CCCTGGAGAAACAGATTGACA-3′ 5′-TACTGGGGAAAGTAGCCTGGT-3′	60
hKCNQ1 (AY114213.1)	154	5′-AACACTGCTGGAAGTGAGCAT-3′ 5′-CATGGGTCGAATGACCTTAAT-3′	60

QRT-PCR, quantitative RT-PCR.

short-circuit current (I_{sc}) were made using monolayers mounted in Ussing chambers (4.5 cm^2) and bathed on both sides with standard saline solution containing (in mM) 130 NaCl, 6 KCl, 1.5 $CaCl_2$, 1 $MgCl_2$, 20 $NaHCO_3$, 0.3 Na H_2PO_4, and 1.3 Na_2HPO_4, pH 7.4, which was maintained at 37°C and bubbled with 95% O_2-5% CO_2. Voltage-clamp experiments were performed between *days 12* and *16* with DVC1000 epithelial voltage-current clamps (WPI), and the data were digitized, stored, and analyzed using Axoscope software (Axon Instruments). For experiments involving measurement of basolateral membrane K^+ current, amphotericin B (15 μM) was used to perforate the apical membrane of monolayers mounted in Ussing chambers. In these experiments the basolateral (extracellular) surface was bathed with (in mM) 120 Na-methanesulfonate, 10 KCl, 20 $NaHCO_3$, 30 mannitol, 1 $MgSO_4$, 1 $CaCl_2$, and 10 glucose (pH 7.4), while the apical (intracellular) side was bathed with (in mM) 120 K-methanesulfonate, 10 NaCl, 20 $KHCO_3$, 30 mannitol, 1 $MgSO_4$, 1 $CaCl_2$, and 10 glucose (pH 7.4). The data were acquired using a Digidata 1322 data acquisition system (Axon Instruments/Molecular Devices, Union City, CA).

Statistics. Statistical significance was determined using an unpaired, two-tailed *t*-test. Statistical significance was accepted at $P < 0.05$.

RESULTS

Identification of P2Y receptors and A_{2b} receptors in primary and immortalized HME cells. Figure 1, *A* and *B*, shows RT-PCR products obtained from primary and immortalized HME cells with specific primers designed to detect human P2Y receptor subtypes. Both primary and immortalized HME cells contained mRNA transcripts for $P2Y_1$, $P2Y_2$, $P2Y_4$, and $P2Y_6$ receptors. In addition, both primary and immortalized HME cells also expressed the A_{2b} subtype of adenosine receptors (Fig. 1, *A* and *B*). Figure 1*C* shows the relative levels of P2Y receptor mRNA expression in immortalized HME cells, using QRT-PCR. The $P2Y_2$ receptor mRNA appeared to be in greatest abundance, whereas the $P2Y_4$ subtype was lowest relative to the other subtypes. Western blot analysis using commercially available antibodies for human $P2Y_1$ and $P2Y_2$ receptors showed several nonspecific bands, thus making it difficult to confirm protein expression using these antibodies (data not shown).

Effects of UTP, UDP + hexokinase, and adenosine 5′-O-(3-thiotriphosphate) on $[Ca^{2+}]_i$ in immortalized HME cells. $[Ca^{2+}]_i$ was measured using fura-2 AM-loaded HME cells following stimulation with adenosine 5′-*O*-(3-thiotriphosphate) (ATPγS), UTP, or UDP + hexokinase (hexokinase was used to degrade any contaminant UTP present in commercially available UDP samples). As shown in Fig. 2*A*, 50 μM UDP + hexokinase, 10 μM UTP, and 50 μM ATPγS all increased $[Ca^{2+}]_i$ in HME cells. Figure 2*B* shows the effects of increasing UTP concentration on the time course of $[Ca^{2+}]_i$ in immortalized HME cells ($n = 23$ cells), and Fig. 2*C* shows the normalized concentration-effect relationships for the UTP- and ATPγS-stimulated Ca^{2+} responses in immortalized HME cells. EC_{50} values for UTP and ATPγS were 4.2 ± 0.1 μM ($n = 23$ cells) and 13.7 ± 0.4 μM ($n = 20$ cells), respectively.

HME cells exhibit basal benzamil-sensitive Na^+ transport. HME cells grown in monolayer culture exhibited a basal I_{sc} that ranged between 8 and 20 μA and a transepithelial resistance between 450 and 520 Ω·cm^2. Addition of benzamil (5 μM) to the apical solution produced a rapid and complete inhibition of the basal I_{sc} (Fig. 3*A*). Both primary and immortalized HME cell monolayers exhibited benzamil-sensitive currents (primary cells: 9.0 ± 1.2 μA vs. immortal cells: 9.7 ± 2.6 μA) that were not significantly different. Concentration-response relationships reported in Fig. 3*B* indicate that benzamil was the most potent inhibitor of the basal I_{sc} with an IC_{50} value of 137 ± 9 nM, followed by amiloride (IC_{50} = 483 ± 37 nM) and incomplete inhibition by methyl isopropyl amiloride at 100 μM. Basolateral addition of 10 μM UTP to monolayers maintained under Cl^- free conditions (where Cl^- was replaced with methanesulfonate) evoked a rapid increase in I_{sc} that returned to baseline levels within 5 min following agonist addition (Fig. 3*C*). The UTP-evoked I_{sc} response under

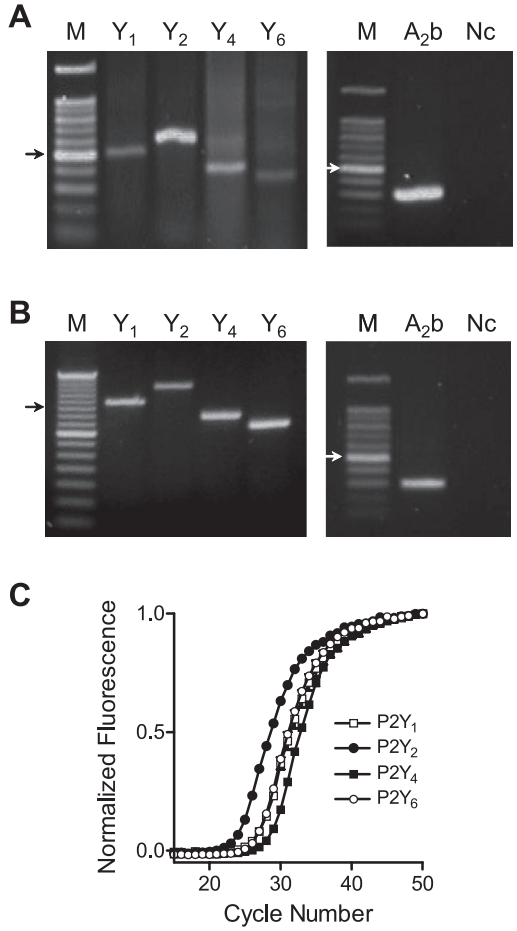

Fig. 1. Detection of P2Y receptors and the A_{2b} adenosine receptor in RNA samples extracted from primary and immortalized human mammary epithelial (HME) cells using RT-PCR. *A*: RT-PCR amplification of human P2Y receptors with RNA isolated from primary HME cells. M, bp markers; Y_1, $P2Y_1$, Y_2, $P2Y_2$, Y_4, $P2Y_4$; Y_6, $P2Y_6$; Nc, negative control performed without RT. Arrows indicate 500 bp. *B*: RT-PCR amplification of human P2Y receptors with RNA isolated from immortalized HME cells. *C*: quantitative RT-PCR (QRT-PCR) showing the relative abundance of P2Y receptor mRNA in immortalized HME cells ($n = 3$ for each receptor subtype). Efficiencies for $P2Y_1$ (0.92), $P2Y_2$ (0.91), $P2Y_4$ (0.98), and $P2Y_6$ (0.96) receptors were determined using the slope of the amplification plots. A single peak melting temperature was obtained for each P2Y receptor PCR product. Primers and their predicted sizes are shown in Tables 1 and 2.

Cl^- free conditions was not significantly different from that observed in normal saline solution.

Effects of hydrocortisone on ENaC subunit mRNA levels in immortalized cells. Figure 4*A* shows the PCR products detected by RT-PCR in immortalized HME cells using primers for ENaC α-,β-, and γ-subunits after 30 cycles. Immortalized cells grown in the presence of hydrocortisone (0.5 μg/ml) exhibited approximately threefold higher levels of mRNA expression for each ENaC subunit compared with cells without hydrocortisone (Fig. 4*B*).

Expression of CFTR in primary and immortalized HME cells. Previous studies have shown that mouse mammary epithelial cells express CFTR and that this channel plays a role in anion secretion (2). Therefore, we examined both primary and immortalized HME cells to see whether we could detect CFTR mRNA. RT-PCR experiments showed relatively lower levels of CFTR mRNA expression in HME cells and MCF-7 cells, a human breast tumor cell line (Fig. 5), compared with expression in human colonic epithelial cells (T84 cells). Treatment with β-estradiol (100 nM) for 96 h did not result in detectable expression of CFTR channel mRNA after 30 cycles in primary or immortalized HME cells (Fig. 5*B*). QRT-PCR

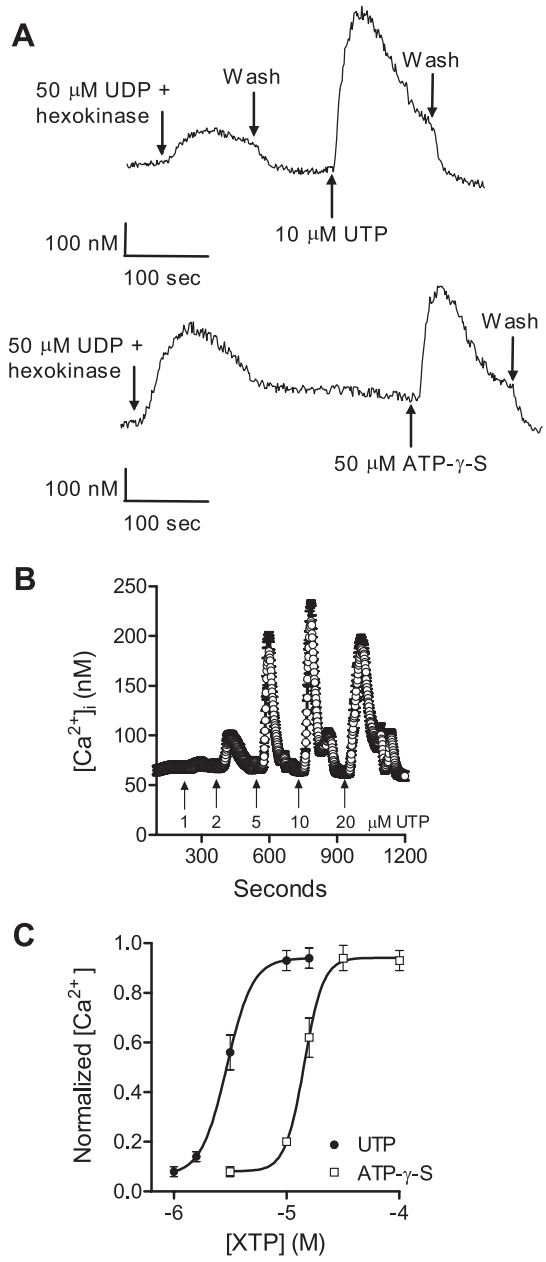

Fig. 2. Effects of UTP, UDP + hexokinase, and adenosine 5′-*O*-(3-thiotriphosphate) (ATPγS) on intracellular Ca^{2+} concentrations ($[Ca^{2+}]_i$) in immortalized HME cells. *A*: UDP + hexokinase (50 μM) and UTP (10 μM) increased $[Ca^{2+}]_i$ in HME cells (*top*). UDP + hexokinase (50 μM) and ATPγS (50 μM) also increased $[Ca^{2+}]_i$ in HME cells (*bottom*). *B*: effects of increasing UTP concentration on the time course of $[Ca^{2+}]_i$ in HME cells ($n = 23$ cells). Note that the cells were washed with HBSS after each addition of UTP. *C*: normalized concentration-effect relationships for the UTP- and ATPγS-stimulated $[Ca^{2+}]_i$ responses in immortalized HME cells. The logistic function $R = Min + \{(Max - Min)/[1 + 10^{(\log X - \log EC_{50})}]\}$ was used to fit the concentration-response data. Hill coefficients were 3.8 ± 0.1 and 5.2 ± 0.4 for UTP and ATPγS respectively. The EC_{50} values were determined from the nonlinear least-squares fit of the data and are reported in RESULTS.

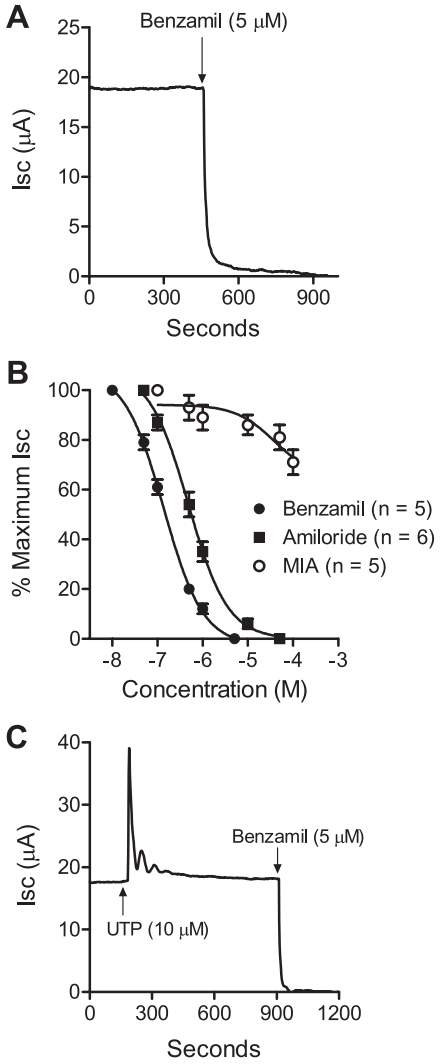

Fig. 3. Effects of Na^+ channel blockers and UTP on HME cell transport function. *A*: immortalized HME cell monolayers exhibited a basal short-circuit current (I_{sc}) that was blocked by apical addition of 5 μM benzamil (tracing is representative of 6 experiments). *B*: concentration-response relationships for benzamil, amiloride, and methyl isopropyl amiloride (MIA) on the basal I_{sc} of immortalized HME cell monolayers bathed in symmetric saline solution (n = 6 for each blocker). The logistic function given in Fig. 3 legend with a Hill slope of −1 was used to fit the data. IC_{50} values are reported in RESULTS. *C*: effects of 10 μM UTP added to the basolateral solution of immortalized HME cell monolayers bathed in symmetric Cl^--free saline solution (tracing is representative of 6 experiments).

experiments comparing CFTR mRNA expression in immortalized HME cells and T84 cells indicated relatively low levels of expression in HME cells compared with T84 cells (Fig. 5*C*).

Apical benzamil inhibits the effect of UTP on I_{sc}. Results reported in Fig. 6, *A*and *B*, show that apical pretreatment of monolayers with 5 μM benzamil for 5 min before addition of UTP (10 μM) inhibited ~83% of the increase in I_{sc} observed in control monolayers. This result suggests that most of the UTP-stimulated increase in current is dependent on apical ENaC channel activity. In addition, a comparison of the basal benzamil-sensitive I_{sc} was made between monolayers cultured in the presence and absence of hydrocortisone. Results presented in Fig. 6*C* show that the basal benzamil-sensitive I_{sc} was significantly increased by ~45% when monolayers were grown in the presence of hydrocortisone. This result suggests that hydrocortisone, presumably acting through glucocorticoid receptors, increases the basal ENaC-dependent I_{sc}.

Effects of BAPTA-AM on the UTP-stimulated I_{sc} response. Figure 7, *A* and *B*, shows the effects of the membrane-permeable calcium-chelating agent BAPTA-AM on UTP-evoked increases in $[Ca^{2+}]_i$ in immortalized HME cells. BAPTA-AM (50 μM) was added to both apical and basolateral solutions 15 min before stimulation with 10 μM UTP. BAPTA-AM produced a decrease in the peak $[Ca^{2+}]_i$ response that was >95% compared with cells that were not treated with BAPTA-AM. In Fig. 7*C* the effects of BAPTA-AM pretreatment on the UTP-evoked increase in I_{sc} are presented. Although BAPTA-AM did not completely abolish the I_{sc} response, it did substantially blunt the initial increase and eliminated the sustained elevation in current observed in monolayers not treated with BAPTA-AM. This result indicates that a major portion of the UTP-stimulated I_{sc} response is dependent on the UTP-evoked increase in $[Ca^{2+}]_i$.

Effects of known KCNN4 inhibitors on the UTP-stimulated I_{sc} response. To investigate the hypothesis that the UTP-activated K^+ conductance was KCNN4, we tested the effects of two known inhibitors of the channel. In Fig. 8, *A* and *B*, the effects of charybdotoxin and clotrimazole pretreatment are presented. Both compounds were added to the basolateral solution 5 min before basolateral stimulation with 10 μM UTP.

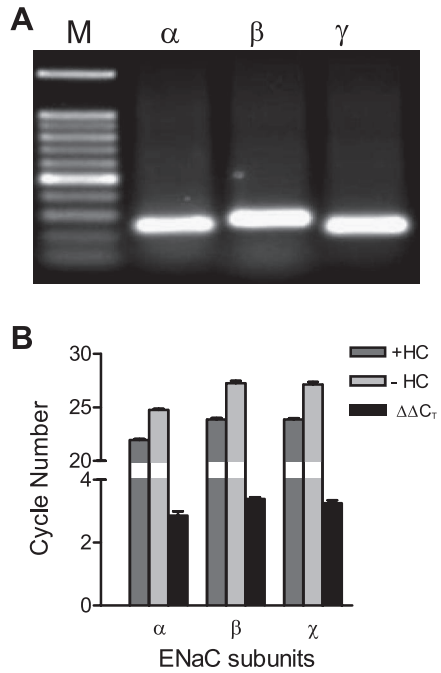

Fig. 4. Expression of epithelial Na^+ channel (ENaC) subunit mRNAs in immortalized HME cells. *A*: RT-PCR products obtained at 30 cycles for each of the ENaC subunits using primer sets described in Table 1. *B*: QRT-PCR results obtained from monolayers grown in the absence and presence of 0.5 μg/ml hydrocortisone (HC). Threshold cycle (C_T) values were determined from amplification plots for each ENaC subunit using MxPro 3000 QPCR analysis software from Stratagene (n = 5). Efficiencies were calculated from the slopes of the amplification plots for α (0.89), β (0.9), and γ (0.9) ENaC subunits. A single peak melting temperature was obtained for each PCR product ($\Delta\Delta C_T$ refers to the difference in C_T values between HC-treated and untreated monolayers after correction for differences in GAPDH expression between HC-treated and untreated samples).

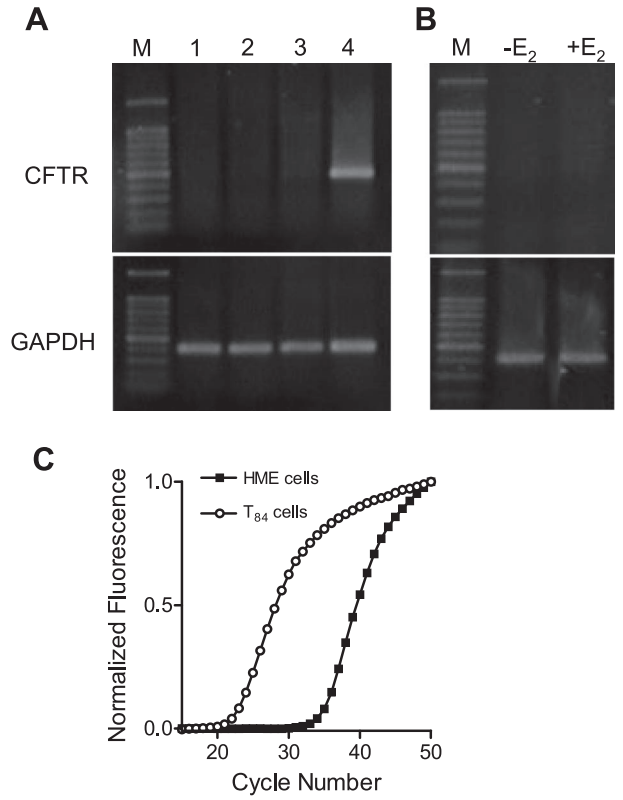

Fig. 5. Expression of CFTR in HME cells. *A*: expression of CFTR in primary HME cells (*lane 1*), immortalized HME cells (*lane 2*), MCF7 cells (*lane 3*), and T84 cells (*lane 4*). RT-PCR amplification of CFTR (30 cycles) was detected in T84 cells but not in primary HME cells, immortalized HME cells, or MCF7 cells. *B*: estrogen (E_2; 100 nM) did not stimulate the expression of CFTR in HME cells. *C*: QRT-PCR data comparing results from T84 cells and immortalized HME cells using the same set of primers as for CFTR. The average C_T values (22 and 33 cycles, respectively) were determined following corrections for differences in GAPDH expression, and a single peak melting temperature was observed for the CFTR PCR product in both cell types ($n = 3$).

Both compounds produced very similar effects that closely resembled the response observed following pretreatment with BAPTA (Fig. 7*C*). The initial I_{sc} response was blunted, and the sustained current was abolished. In a follow-up experiment, the apical membrane of the monolayer was permeabilized with the pore-forming antibiotic amphotericin B so that a K^+ gradient could be imposed across the basolateral membrane while the voltage was clamped at 0 mV. Basolateral pretreatment with 10 μM clotrimazole for 5 min reduced the initial current increase and abolished the sustained current response consistent with the results reported in Fig. 8, *A* and *B*. Measurement of the net change transfer occurring within the first 600 s immediately following UTP addition is shown in Fig. 8*D*. Significant inhibition was observed in monolayers pretreated with either charybdotoxin or clotrimazole compared with vehicle-treated monolayers.

Identification of KCNN4 mRNA. QRT-PCR was used to detect the expression of KCNN4 and KCNQ1 mRNA in total RNA samples from immortalized HME cells. KCNN4 was detected at a threshold cycle (C_T) of 23 cycles, whereas KCNQ1 mRNA appeared to be present in much lower abundance with a C_T of 34 cycles (Fig. 9). These results indicate that KCNN4 mRNA was present in immortalized HME cells at levels similar to those of ENaC channels in HME cells and CFTR in T84 cells.

DISCUSSION

Several mammalian subtypes of P2Y receptors ($P2Y_1$, $P2Y_2$, $P2Y_4$, $P2Y_6$, $P2Y_{11}$, $P2Y_{12}$, $P2Y_{13}$, and $P2Y_{14}$) have been cloned and functionally characterized (4, 6, 7, 18, 28). Among these receptors, $P2Y_1$, $P2Y_2$, $P2Y_4$, $P2Y_6$, and $P2Y_{11}$ couple to $G_{q/11}$ and activate phospholipase C, resulting in increased inositol 1,4,5-trisphosphate formation and mobilization of intracellular Ca^{2+} (2, 5, 8, 12, 14, 15, 27, 29, 29). In the present study, several P2Y receptor mRNA subtypes ($P2Y_1$, $P2Y_2$ $P2Y_4$, and $P2Y_6$) were identified in HME cells. Calcium imaging experiments showed that stimulation of HME cells with P2Y receptor agonists produced increases in $[Ca^{2+}]_i$. Concentration-response relationships for UTP and ATPγS along with experiments with UDP provided functional evidence for multiple P2Y receptor subtypes present in these cells.

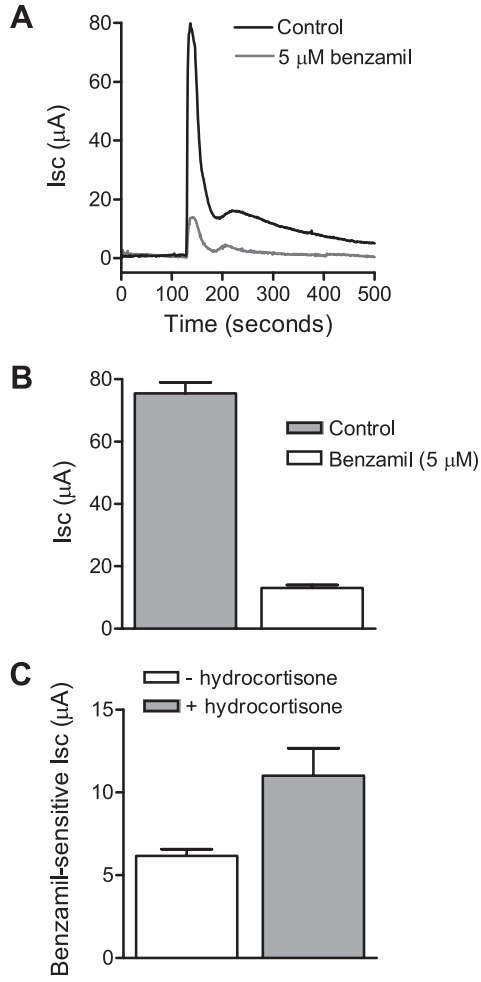

Fig. 6. Pretreatment of monolayers with apical benzamil (5 μM) inhibits the UTP-stimulated increase in I_{sc}. *A*: representative traces showing the effects of UTP on I_{sc} in control and benzamil-treated monolayers. Note that the basal currents were normalized to 0 mV for benzamil-treated and untreated monolayers, allowing for a direct comparison of the UTP-stimulated I_{sc} response. *B*: comparison of peak UTP responses in the presence and absence of apical 5 μM benzamil (control, $n = 6$; benzamil treated, $n = 9$). *C*: basal benzamil-sensitive I_{sc} measurements obtained from monolayers grown in the absence and presence of 0.5 μg/ml HC (−HC, $n = 6$; +HC, $n = 9$).

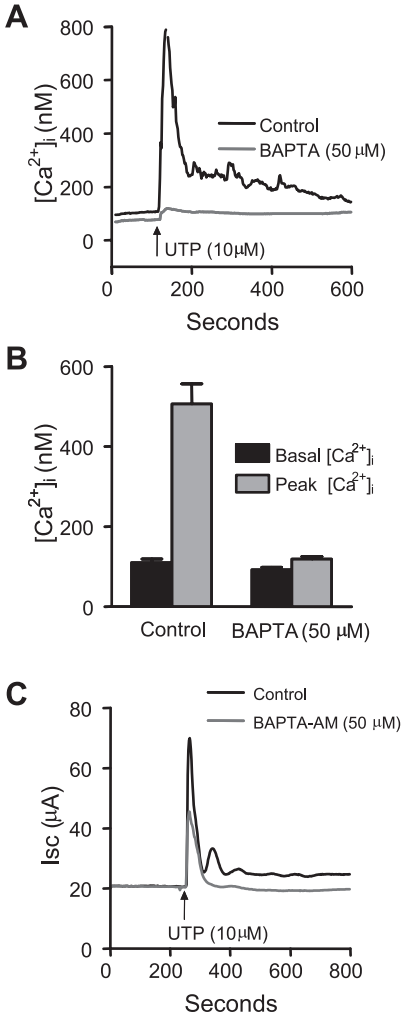

Fig. 7. Effects of UTP on $[Ca^{2+}]_i$ and I_{sc} in immortalized HME cells. *A*: pretreatment with 50 μM BAPTA-AM significantly blocked the UTP-stimulated increase in $[Ca^{2+}]_i$ (tracing shows averaged responses from 20 cells). *B*: analysis of $[Ca^{2+}]_i$ peak responses before and after treatment with BAPTA-AM ($n = 5$). *C*: representative data from paired experiments comparing the effects of basolateral UTP (10 μM) on monolayers pretreated with BAPTA-AM and a vehicle (DMSO)-treated control (representative of 6 experiments). Mean differences between the basal I_{sc} and the plateau I_{sc} at 400 s after UTP in the absence and presence of BAPTA-AM were 5 ± 0.8 and 0.3 ± 0.5 μA, respectively.

RT-PCR also revealed that HME cells express A_{2b} adenosine receptor mRNA, which has been shown to be coupled to G_s and to activate adenylyl cyclase (20).

Previous studies of human mammary tumor cells (MCF-7) and mouse mammary epithelial cells (31EG4 cells) showed that increases in $[Ca^{2+}]_i$ elicited by purinergic receptor agonists did stimulate Cl^- secretion (3, 10, 22). P2Y receptor agonists including ATP, UTP, and ADP increased $[Ca^{2+}]_i$ and anion efflux that was inhibited by DIDS in MCF-7 cells (10). In mouse mammary epithelial cells, $P2Y_2$ receptors were identified by RT-PCR, and stimulation of Ca^{2+}-activated Cl^- channels was detected following treatment with ATP or UTP. Cl^- channel activation produced a rapid depolarization of the apical membrane consistent with Cl^- efflux and transepithelial Cl^- secretion (3). CFTR expression and activity also was observed in mouse mammary epithelial cells and was involved

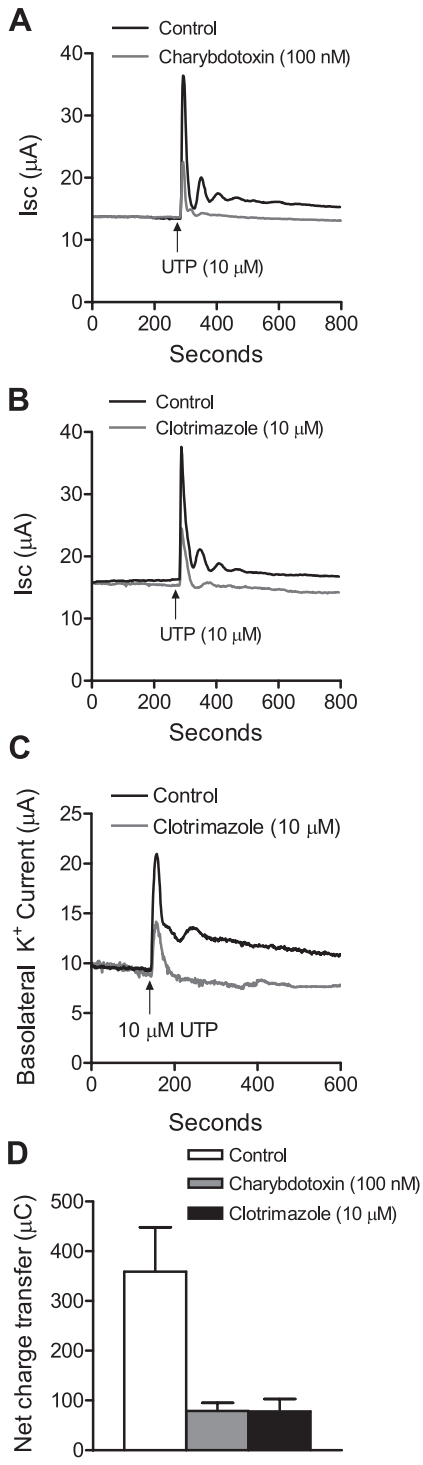

Fig. 8. Effects of KCNN4 channel blockers on the UTP-activated I_{sc} response. *A*: representative traces from experiments comparing monolayers pretreated with 100 nM charybdotoxin and a vehicle (saline)-treated control (representative of 6 experiments). *B*: representative tracings comparing monolayers pretreated with 10 μM clotrimazole and a vehicle (DMSO)-treated control (representative of 6 experiments). *C*: representative traces comparing apical membrane amphotericin B-treated monolayers pretreated with clotrimazole and a vehicle (DMSO)-treated control (representative of 4 experiments). Note that the basolateral membrane was held at 0 mV and that an outwardly directed K^+ concentration gradient was imposed (see MATERIALS AND METHODS for ionic composition of apical and basolateral solutions). *D*: net charge transfer calculated from the I_{sc} traces (see *A* and *B*) over a 600-s interval immediately following the UTP-evoked increase in I_{sc} ($n = 6$ monolayers for each condition).

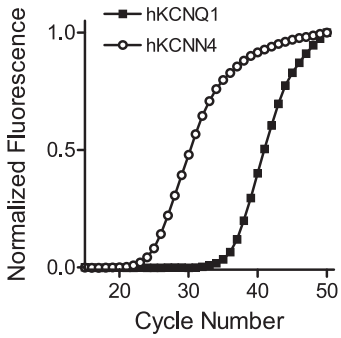

Fig. 9. QRT-PCR data showing the relative abundance of KCNN4 mRNA compared with KCNQ1 mRNA. The average C_T values were 23 and 34 cycles, respectively ($n = 3$ for each), and a single peak melting temperature was obtained for each PCR product. Efficiencies for KCNQ1 and KCNN4 were 0.96 and 0.87, respectively.

in Cl^- efflux and fluid secretion across the epithelium (2, 29). Similarly, forskolin stimulation of bovine mammary epithelial cells produced an increase in I_{sc} that was blocked by *N*-(4-methyphenylsulfonyl)-*N*′-(4-trifluoromethylphenyl) urea, a known inhibitor of CFTR Cl^- channel activity (27). In the present study, CFTR mRNA was detected in HME cells at relatively low levels compared with T84 cells, which served as a positive control. Attempts to stimulate CFTR expression with estrogen were not successful, although previous studies in rat endometrial epithelial cells showed that CFTR mRNA expression was enhanced following estrogen treatment (25, 26).

Basal ENaC-dependent Na^+ transport was previously characterized in 31EG4 cells, indicating that this mouse mammary epithelial cell line is capable of both Na^+ absorption and anion secretion (2). In addition, an amiloride-sensitive component to the I_{sc} was observed in bovine mammary epithelial cells following treatment with dexamethasone, suggesting that ENaC activity was subject to regulation by glucocorticoids (27). In the present study, RT-PCR revealed that HME cells express ENaC α-, β-, and γ-subunit mRNAs. Moreover, transport experiments indicated that the basal I_{sc} was blocked by amiloride analogs with IC_{50} values and a rank order of potency consistent with ENaC-dependent electrogenic Na^+ absorption. Growing immortalized HME cells in the presence of hydrocortisone resulted in an increase in expression of all three ENaC subunits and increased the basal benzamil-sensitive I_{sc}. This response was consistent with the previously described effects of dexamethasone on ENaC activity in bovine mammary epithelial cells (27).

Basolateral stimulation with UTP produced an increase in I_{sc} that exhibited oscillations that lasted for several minutes. However, unlike the effects of UTP observed in mouse mammary epithelial cells and human MCF-7 cells, the I_{sc} increase in HME cells was not Cl^- dependent, and most of the response was inhibited by apical addition of benzamil (3, 10). This result does not exclude the possibility that UTP may stimulate HCO_3^- secretion, and this could contribute to the benzamil-insensitive I_{sc} response. Chelating intracellular Ca^{2+} with BAPTA-AM as a means to significantly reduce the increase in $[Ca^{2+}]_i$ produced by UTP substantially altered both the magnitude and duration of the initial I_{sc} response, providing evidence that a major portion of the transport-related actions of UTP were dependent on $[Ca^{2+}]_i$. Concentration-response relationships for UTP and ATPγS revealed Hill coefficients that suggested a high degree of amplification with respect to Ca^{2+} mobilization, perhaps through Ca^{2+}-induced Ca^{2+} release, activation of multiple P2Y receptor subtypes, or some combination of these factors. Although increases in $[Ca^{2+}]_i$ appear to be important, the I_{sc} response was not completely abolished after pretreatment with BAPTA-AM, suggesting that Ca^{2+}-independent mechanisms also may be involved.

Partial inhibition of the UTP-evoked I_{sc} also was produced by basolateral charybdotoxin and clotrimazole at concentrations that are known to block KCNN4 K^+ channels (1, 16, 21, 28, 30). Moreover, clotrimazole was shown to inhibit the increase in basolateral membrane K^+ current consistent with the observed effects on I_{sc} and with inhibition of Ca^{2+}-activated K^+ channels. QRT-PCR analysis demonstrated that HME cells expressed KCNN4 mRNA and that the relative level of mRNA expression was greater than that for the KCNQ1 K^+ channel. Interestingly, the results obtained in the present study are similar to those of a previous report involving CFT1 airway epithelial cells, where activation of a clotrimazole-sensitive K^+ conductance in the basolateral membrane produced a significant increase in amiloride-sensitive Na^+ transport (13). Activation of basolateral K^+ channels such as KCNN4 would be expected to produce membrane hyperpolarization, thus increasing the driving force for Na^+ uptake across the apical membrane and, consequently, net transepithelial Na^+ transport across the epithelium.

Although the precise origin (duct cells vs. lobular acinar cells) of HME cells described in this study is not known, we speculate that, based on the age of the donor, low levels of CFTR expression, and the existence of ENaC-dependent Na^+ transport, the cells exhibit duct-type transport phenotype. We observed that both primary and immortal HME cells expressed several P2Y receptor subtypes ($P2Y_1$, $P2Y_2$ $P2Y_4$, and $P2Y_6$) that bind UTP, UDP and ATP to produce mobilization of intracellular Ca^{2+}. The expression of multiple P2Y receptor subtypes and the presence of A_{2b} adenosine receptors indicate

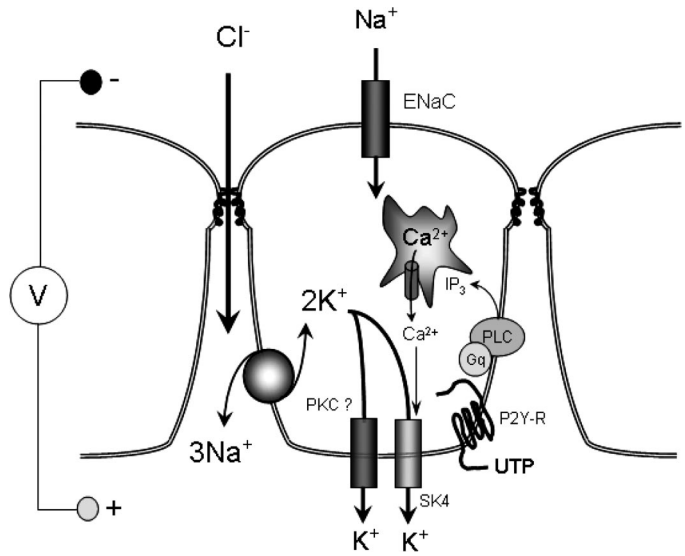

Fig. 10. A cell model summarizing the proposed mechanism for basolateral UTP stimulation of Na^+ transport in HME cells. A description is presented in the DISCUSSION. PLC, phospholipase C, G_q, G protein α-subunit; IP_3, inositol 1,4,5-trisphosphate; P2Y-R, P2Y receptor.

that HME cells are capable of responding to wide array of purinergic signaling molecules. In contrast to other mammary epithelia that exhibit anion secretion or a combination of anion secretion and ENaC-dependent Na^+ absorption, both primary and immortal HME cells form monolayers that primarily exhibit electrogenic Na^+ absorption. A model summarizing the effects of basolateral UTP on Na^+ transport in HME cells is presented in Fig. 10. Stimulation of HME cells with UTP enhances Na^+ transport by activation of basolateral K^+ channels that are Ca^{2+}-dependent and possess pharmacological properties characteristic of KCNN4 K^+ channels. In addition, our results suggest that UTP activates a Ca^{2+}-independent K^+ channel in the basolateral membrane that contributes to the initial increase in I_{sc} observed immediately after P2Y receptor stimulation. We speculate that this channel may be regulated by PKC, but its molecular identity remains to be determined.

ACKNOWLEDGMENTS

We thank Katie Schiller for technical assistance with the PCR experiments.

GRANTS

This work was partly supported by Korea Research Foundation Grant KRF-005-E00076 (to S. Y. Lee) and National Institutes of Health Grants AI-50494 and DK-74010 (to S. M. O'Grady).

REFERENCES

1. **Bernard K, Bogliolo S, Soriani O, Ehrenfeld J.** Modulation of calcium-dependent chloride secretion by basolateral SK4-like channels in a human bronchial cell line. *J Membr Biol* 196: 15–31, 2003.
2. **Blaug S, Hybiske K, Cohn J, Firestone GL, Machen TE, Miller SS.** ENaC- and CFTR-dependent ion and fluid transport in mammary epithelia. *Am J Physiol Cell Physiol* 281: C633–C648, 2001.
3. **Blaug S, Rymer J, Jalickee S, Miller SS.** P2 purinoceptors regulate calcium-activated chloride and fluid transport in 31EG4 mammary epithelia. *Am J Physiol Cell Physiol* 284: C897–C909, 2003.
4. **Boeynaems JM, Communi D, Gonzalez NS, Robaye B.** Overview of the P2 receptors. *Semin Thromb Hemost* 31: 139–149, 2005.
5. **Burnstock G.** Purinergic signaling and vascular cell proliferation and death. *Arterioscler Thromb Vasc Biol* 22: 364–373, 2002.
6. **Burnstock G.** Introduction: P2 receptors. *Curr Top Med Chem* 4: 793–803, 2004.
7. **Burnstock G, Knight GE.** Cellular distribution and functions of P2 receptor subtypes in different systems. *Int Rev Cytol* 240: 31–304, 2004.
8. **Communi D, Janssens R, Suarez-Huerta N, Robaye B, Boeynaems JM.** Advances in signalling by extracellular nucleotides. The role and transduction mechanisms of P2Y receptors. *Cell Signal* 12: 351–60, 2000.
9. **Fata JE, Werb Z, Bissell MJ.** Regulation of mammary gland branching morphogenesis by the extracellular matrix and its remodeling enzymes. *Breast Cancer Res* 6: 1–11, 2004.
10. **Flezar M, Heisler S.** P2-purinergic receptors in human breast tumor cells: coupling of intracellular calcium signaling to anion secretion. *J Pharmacol Exp Ther* 265: 1499–510, 1993.
11. **Franke WW, Appelhans B, Schmid E, Freudenstein C, Osborn M, Weber K.** Identification and characterization of epithelial cells in mammalian tissues by immunofluorescence microscopy using antibodies to prekeratin. *Differentiation* 15: 7–25, 1979.
12. **Furuya K, Enomoto K, Yamagishi S.** Spontaneous calcium oscillations and mechanically and chemically induced calcium responses in mammary epithelial cells. *Pflügers Arch* 422: 295–304, 1993.
13. **Gao L, Yankaskas JR, Fuller CM, Sorscher EJ, Matalon S, Forman HJ, Venglarik CJ.** Chlorzoxazone or 1-EBIO increases Na^+ absorption across cystic fibrosis airway epithelial cells. *Am J Physiol Lung Cell Mol Physiol* 281: L1123–L1129, 2001.
14. **Harden TK, Boyer JL, Nicholas RA.** P2-purinergic receptors: subtype-associated signaling responses and structure. *Annu Rev Pharmacol Toxicol* 35: 541–579, 1995.
15. **Katoh K, Komatsu T, Yonekura S, Ishiwata H, Hagino A, Obara Y.** Effects of adenosine 5′-triphosphate and growth hormone on cellular H^+ transport and calcium ion concentrations in cloned bovine mammary epithelial cells. *J Endocrinol* 169: 381–388, 2001.
16. **Khanna R, Roy L, Zhu X, Schlichter LC.** K^+ channels and the microglial respiratory burst. *Am J Physiol Cell Physiol* 280: C796–C806, 2001.
17. **Kim H, Farris J, Christman SA, Kong BW, Foster LK, O'Grady SM, Foster DN.** Events in the immortalizing process of primary human mammary epithelial cells by the catalytic subunit of human telomerase. *Biochem J* 365: 765–772, 2002.
18. **Leipziger J.** Control of epithelial transport via luminal P2 receptors. *Am J Physiol Renal Physiol* 284: F419–F432, 2003.
19. **Medina D.** Mammary developmental fate and breast cancer risk. *Endocr Relat Cancer* 12: 483–495, 2005.
20. **Moro S, Gao ZG, Jacobson KA, Spalluto G.** Progress in the pursuit of therapeutic adenosine receptor antagonists. *Med Res Rev* 26: 131–159, 2006.
21. **Ohya S, Kimura S, Kitsukawa M, Muraki K, Watanabe M, Imaizumi Y.** SK4 encodes intermediate conductance Ca^{2+}-activated K^+ channels in mouse urinary bladder smooth muscle cells. *Jpn J Pharmacol* 84: 97–100, 2000.
22. **Palmer ML, Lee SY, Carlson D, Fahrenkrug S, O'Grady SM.** Stable knockdown of CFTR establishes a role for the channel in P2Y receptor-stimulated anion secretion. *J Cell Physiol* 206: 759–770, 2006.
23. **Palmer ML, Lee SY, Maniak PJ, Carlson D, Fahrenkrug SC, O'Grady SM.** Protease-activated receptor regulation of Cl^- secretion in Calu-3 cells requires prostaglandin release and CFTR activation. *Am J Physiol Cell Physiol* 290: C1189–C1198, 2006.
24. **Parmar H, Cunha GR.** Epithelial-stromal interactions in the mouse and human mammary gland in vivo. *Endocr Relat Cancer* 11: 437–458, 2004.
25. **Rochwerger L, Buchwald M.** Stimulation of the cystic fibrosis transmembrane regulator expression by estrogen in vivo. *Endocrinology* 133: 921–930, 1993.
26. **Rochwerger L, Dho S, Parker L, Foskett JK, Buchwald M.** Estrogen-dependent expression of the cystic fibrosis transmembrane regulator gene in a novel uterine epithelial cell line. *J Cell Sci* 107: 2439–2448, 1994.
27. **Schmidt CR, Carlin RW, Sargeant JM, Schultz BD.** Neurotransmitter-stimulated ion transport across cultured bovine mammary epithelial cell monolayers. *J Dairy Sci* 84: 2622–2631, 2001.
28. **Schreiber R, Kunzelmann K.** Purinergic P2Y6 receptors induce Ca^{2+} and CFTR dependent Cl^- secretion in mouse trachea. *Cell Physiol Biochem* 16: 99–108, 2005.
29. **Selvaraj NG, Omi E, Gibori G, Rao MC.** Janus kinase 2 (JAK2) regulates prolactin-mediated chloride transport in mouse mammary epithelial cells through tyrosine phosphorylation of Na^+-K^+-$2Cl^-$ cotransporter. *Mol Endocrinol* 14: 2054–2065, 2000.
30. **Takahata T, Hayashi M, Ishikawa T.** SK4/IK1-like channels mediate TEA-insensitive, Ca^{2+}-activated K^+ currents in bovine parotid acinar cells. *Am J Physiol Cell Physiol* 284: C127–C144, 2003.
31. **Woodward WA, Chen MS, Behbod F, Rosen JM.** On mammary stem cells. *J Cell Sci* 118: 3585–3594, 2005.